Nat Biotechnol. Author manuscript; available in PMC 2014 April 21.

Published in final edited form as:
Nat Biotechnol. 2012 September ; 30(9): 876–882. doi:10.1038/nbt.2328.

Directed differentiation of human pluripotent stem cells into mature airway epithelia expressing functional CFTR protein

Amy P. Wong[1,2], **Christine E. Bear**[3], **Stephanie Chin**[3], **Peter Pasceri**[1], **Tadeo O. Thompson**[2], **Ling-Jun Huan**[3], **Felix Ratjen**[4,5], **James Ellis**[1,2,6], and **Janet Rossant**[1,6,7]

[1]Program in Developmental & Stem Cell Biology, Hospital for Sick Children, Toronto, ON, M5G 1L7

[2]Ontario Human Induced Pluripotent Stem Cell Facility, Toronto, ON, M5G 1L7

[3]Program in Molecular Structure and Function, Hospital for Sick Children, Toronto

[4]Program in Physiology & Experimental Medicine, Hospital for Sick Children, Toronto

[5]Division of Respiratory Medicine, Hospital for Sick Children, Toronto

[6]Department of Molecular Genetics, University of Toronto, Toronto, ON, M5S 1A8

[7]Department of Obstetrics and Gynaecology, University of Toronto, Toronto

Abstract

Cystic fibrosis (CF) is a fatal genetic disease caused by mutations in the *CFTR* (cystic fibrosis transmembrane conductance regulator) gene that regulates chloride and water transport across all epithelia and affects multiple organs including the lungs. Here we report an *in vitro* directed differentiation protocol for generating functional CFTR-expressing airway epithelia from human embryonic stem cells. Carefully timed treatment by exogenous growth factors that mimic endoderm developmental pathways *in vivo* followed by air-liquid interface culture results in maturation of patches of tight junction-coupled differentiated airway epithelial cells that demonstrate active CFTR transport function. As a proof-of-concept, treatment of CF patient induced pluripotent stem cells (iPSC)-derived epithelial cells with a novel small molecule compound to correct for the common CF-processing mutation resulted in enhanced plasma membrane localization of mature CFTR protein. Our study provides a method for generating patient-specific airway epithelial cells for disease modeling and *in vitro* drug testing.

Please address inquiries to: Janet Rossant, Hospital for Sick Children, 555 University Avenue, Toronto, Ontario, Canada M5G 1X8, Phone: 416-813-7929, Fax: 416-813-5085, janet.rossant@sickkids.ca Or James Ellis, Hospital for Sick Children, 101 College Street, TMDT @ MaRS 13-710, Toronto, Ontario, Canada M5G 1L7, Phone: 416-813-7295, Fax: 416-813-5252, jellis@sickkids.ca.

Competing Interests Statement
The authors declare that they have no competing financial interests.

Supplementary Information is linked to the online version of the paper at www.nature.com/nature.

Author contributions: A.P.W, J.R, J.E, C.B, and F.R conceived the study and experimental design. A.P.W performed and analyzed experiments and wrote the manuscript. C.B, P.P, T.O.T, LJ.H, S.C, and F.R provided reagents, conceptual and/or technical support in generating iPSC lines, teratoma assay, iodide efflux measurements. All authors edited and approved the final manuscript.

Efforts to differentiate hESC into lung epithelia have generated cells that express distal airway epithelial phenotypes expressing surfactant protein-C[1–3]. These reports relied on spontaneous mixed-lineage embryoid bodies to differentiate hESC directly into lung endoderm with low efficiency and generated mostly cells expressing distal alveolar markers. A recent study show a stepwise generation of lung endoderm progenitors from human induced pluripotent stem cells (iPSC) but failed to generate mature proximal and distal lung epithelial phenotypes[4]. To date, no studies have been able to generate proximal conducting airway epithelia with functional polarized CFTR. Therefore, we developed a method to recapitulate the sequential processes that progressively restrict progenitor cells from endoderm to proximal lineage-specific lung epithelia[5,6] and were able to generate functional proximal conducting airway epithelia expressing CFTR from human pluripotent stem cells.

Since lung forms from definitive endoderm, we first differentiated hESC towards definitive endoderm using a previously described method[7], based on developmental pathways of endoderm formation at gastrulation[6]. Treatment with Activin-A and WNT3A for 4 days is sufficient to induce a large percentage of cells into definitive endoderm as determined by co-expression of CXCR4 and cKIT, and the endoderm transcription factors FOXA2 and SOX17 (Supplementary Fig. 1 online).

After gastrulation, anterior-posterior signals pattern the primitive gut tube into distinct regions[6]. The developing cardiac mesoderm patterns the anterior ventral foregut endoderm through secretion of the fibroblast growth factor-2 (FGF2)[8]. High concentration of FGF2 induces a *NKX2.1* expression domain typical of the early lung endoderm[9]. Sonic hedgehog (SHH) signaling promotes embryonic lung growth and suppresses pancreatic development[10,11]. Thus, to promote anterior foregut identity and specify lung cell fate, definitive endoderm cells were treated with FGF2 and SHH (Supplementary Fig. 2 online). After 5 days of exposure, 85% of the cells expressed the pan-endoderm transcription factor FOXA2. The majority (78%) of the cells co-expressed the pan-epithelial marker EpCAM and the transcription factor *NKX2.1*. Up-regulation of anterior foregut endoderm transcription factors *SOX2* and *NKX2.1* as well as pharyngeal endoderm marker *FOXG1,*and thyroid markers *TG* and *PAX9* was observed by RT-PCR. The posterior hindgut marker *CDX2* was not detected. *NKX2.1* is a good marker for lung endoderm but is also expressed in the thyroid and forebrain[12]. Although other thyroid markers were seen, importantly, the ectoderm marker *PAX6* was also not detected which excludes the possibility of forebrain-derived *NKX2.1* expression. The definitive endoderm marker *SOX17* was down-regulated but some expression of transcription factors indicative of liver, *HNF4,* and pancreas, *NKX6.1* and *PDX1,* were detected, suggesting that other endoderm lineages were also present. Nonetheless FGF2 and SHH can efficiently induce anterior foregut derivatives from definitive endoderm.

Gain- and loss-of-function studies in mouse embryonic lung organ cultures, combined with studies in null and transgenic mouse lines, have identified specific growth factors important for lung development from the NKX2.1-expressing endoderm[5] including FGF and BMP4. FGF10 is a key growth factor expressed by the mesenchyme at the earliest stage of lung development and stimulates lung bud outgrowth and organogenesis[13]. FGF7, also expressed by the mesenchyme, is mainly involved in stimulating fluid secretion in the lungs but has a

role in epithelial cell growth[14]. We found that the combination of FGF7 and FGF10 at 50ng/ml augmented expression of the transcription factors *NKX2.1* and *FOXA2* compared to definitive endoderm levels (Supplementary Fig. 3 online). As the lung bud actively branches, the bud stalk (future conducting airways) matures in an environment where signals that drive bud tip outgrowth are reduced or repressed[15]. High concentrations of BMP4 stimulate a distal cell fate while low concentration of BMP4 promote a proximal cell fate[16]. Retinoic acid (RA) signaling up-regulates FGF10 in the developing lung mesenchyme to stimulate lung bud outgrowth[17] but it also plays a key role in inducing alveolar epithelial cell fate and surfactant production during the later phase of lung development[18]. Therefore to enhance proximal airway fate and suppress distal cell fate, cultures were incubated with varying levels of BMP4 and in the absence of RA. The ES-derived anterior foregut cells were exposed to FGF10, FGF7 and varying concentrations of BMP4 to determine the optimal concentration of BMP4 that would induce proximal cell fate (Fig. 1a,b). RT-PCR showed that low concentrations of BMP4 induced up-regulation of airway cell markers such as *KRT5* and *Trp63* (P63, basal cell marker), *FOXJ1* and *SOX17* (ciliated cell markers), *NKX2.1*, *CFTR* and the pan-endoderm marker *FOXA2* (Fig 1c). Another airway marker, *MUC5AC* (goblet cell marker), was not detected. In addition, the distal Type II alveolar cell marker surfactant protein-C (SFTPC) and Clara cell secretory marker *SCGB1A1* (more abundant in the smaller conducting airways) were not detected. *SOX9*, a distal tip marker found in the developing lung bud, was also detected. Therefore, a combination of FGF7, FGF10 and low concentration of BMP4 can induce up-regulation of some conducting airway cell lineages from anterior foregut endoderm.

To further promote airway differentiation, FGF18 which enhances proximal but not distal airway formation and plays a role in increasing the size of the conducting airways following maturation of the epithelium[19] was added (Fig 2a,b). Further up-regulation of airway genes *KRT5*, *Trp63*, *FOXJ1*, *SOX17*, *MUC5AC*, *CFTR*, lower levels of *SCGB1A1*, and no significant detection of *SFTPC* (Fig. 2c). The transcription factors *NKX2.1* and *FOXA2* and the distal tip progenitor marker *SOX9* were down regulated. Relative to their adult tissue counterparts, other endoderm lineage markers *AFP* (liver), *PDX1* (pancreas), *TG* (thyroid) and *PAX9* (pharyngeal endoderm) were not detected at this stage. Moreover, flow cytometric quantification revealed cells that expressed pan-cytokeratin (panKRT, 33%) CFTR (30%), FOXJ1 (36%), NKX2.1 (32%) (Fig. 2d) suggesting that at least one-third of the cells in the culture are of the ciliated CFTR-expressing airway phenotype. Over 50% of the cells were P63+ suggesting the vast majority of the cells are potentially basal cell progenitors, previously shown to give rise to other proximal airway lineages[20]. Significant cell proliferation, as measured by BrdU incorporation, occurred during the first 14 days of differentiation and declined by the late proximal specification stage (D19, Figure 2e,f). The increased expression of proximal lineage markers on Day 19 is consistent with the reduction in cell proliferation as differentiation progressed. Collectively, our data support a mechanism for airway development where FGF7, FGF10, BMP4 and FGF18 are required to promote airway lineage development.

Importantly, this method of directed differentiation was broadly applicable to several pluripotent cell lines with varying efficiencies (Supplementary Fig. 4 online). During the early stages of differentiation, up-regulated expression of the early lung marker *NKX2.1* was

variable between the hESC lines. Similarly, differentiation of several wild-type iPSC and CF iPSC lines also show varying efficiencies in lung marker expression (Supplementary Fig. 5 online). This suggests that optimization of the differentiation protocol may be required to reflect line-to-line variability.

To further develop and mature the cells towards functional airway epithelium *in vitro,* we employed commercially available media that support the growth and differentiation of primary bronchial epithelial cells *ex vivo* along with air-liquid interface (ALI) to mimic the post-natal airway epithelial niche *in vivo* and promote differentiation, maturation and polarization of the epithelium (Fig. 3a). After 5 weeks of ALI, flow cytometry revealed at least 50% of the CFTR+ cells that co-expressed panKRT, FOXJ1 and LHS28 (basal bodies of cilia) indicating an enrichment of cells typical of the ciliated epithelium (Fig. 3b). A dramatically reduced percentage (5%) of cells expressing P63 (an airway progenitor cell marker[20]) was observed (Supplementary Fig. 6 online) suggesting the putative P63+ basal progenitor cells may have differentiated into other airway epithelial lineages as has been previously shown[21]. In addition, the majority of the cells express other conducting airway epithelia markers (Acetylated TUBA1A, cilia), MUC1 (Goblet cell), KRT14 (Basal epithelia) and the pan-endoderm marker FOXA2. A smaller percentage (15%) of cells expressed the transcription factor NKX2.1, which in later stages of lung development regulates Clara cell and Type II alveolar cell differentiation[22]. No cells positive for the pancreatic ductal epithelia marker Hpd1 were found, excluding the possibility that pancreatic ductal epithelial cells are the source of CFTR. Large airway epithelium was established as indicated by protein expression of mucin 16 (a marker of the tracheal epithelium[23]) and cytokeratin 16[24] (Supplementary Fig. 7 online). Gene expression analysis by real-time RT-PCR showed up-regulation of proximal airway lineage markers (*SOX17, FOXJ1, MUC5AC, Trp63, KRT5, ARG2, SOX2*, *CFTR, KRT16, MUC16, NGFR*) comparable or higher than levels in total adult lung or tracheal tissue (Fig. 3c). Clara cell marker *SCGB1A1* and alveolar epithelial cell markers *SFTPC, Pdpn*, *P2X7* and the transcription factors *NKX2.1*, *FOXA2, FOXA1, SOX9* were only observed at very low levels (Supplementary Fig. 8 online). Low levels of the thyroid markers *TG, PAX9*, liver markers *HNF4*, *AFP*, and pancreas marker *PDX1* were also detected (Supplementary Fig. 9 online) suggesting the maturation of the lung lineages remained heterogeneous with other endoderm lineages also present. With the exception of *PITX3*, the other esophageal markers *DLX3* and *MUC2* were not detected. The stratified epithelial marker mainly expressed in the skin *KRT15,* was also detected. However, no expression of the neuronal lineage marker, *PAX6,* and the forebrain marker *FOXG1,* were observed. Immunofluorescence staining and confocal analysis of 5 week old ALI cultures showed contiguous patches of epithelial cells typified by membrane expression of Zona Occludin-1 (ZO1), a protein associated with tight-junctions, and co-staining with pan-KRT (Fig 3d) and CFTR (Fig. 3e). Reconstructed confocal stacked images show apical plasma membrane localization of CFTR (green) (Fig. 3f). Stained sections of the cultures show ciliated cells (3g, H&E) confirmed with antibody staining for cilia (beta IV tubulin, green) and apically-localized CFTR (orange) (Figure 3h high, 3i low magnification respectively). In addition, the cultures stained positive for MUC5AC on the surface of the cells indicative of mucin production (Figure 3j). These

findings suggest air liquid interface can induce maturation and polarization of a ciliated large airway epithelium with proper localization of the CFTR protein.

Directed differentiation of CF mutant iPSC into airway epithelial cells holds great promise for disease modeling and drug discovery. The most common CF mutation (~70% of cases[25]) is caused by a phenylalanine deletion at position 508 (F508del). We generated CF-iPSC lines from three F508del subjects by reprogramming primary human fibroblasts using retroviruses containing the four pluripotency factors (OCT4, KLF4, C-MYC and SOX2) as previously described[26]. Genotype analysis was performed to confirm that the reprogrammed cells carried the F508del homozygous mutation (Supplementary Fig. 10 online). CF-iPSC lines expressed pluripotency markers TRA1-81, TRA1-60 and NANOG, up-regulated expression of endogenous pluripotency genes *OCT4, SOX2, KLF4* and *C-MYC*, and silenced the reprogramming retroviral transgenes, a hallmark of pluripotent stem cells (Supplementary Fig. 11 online). *In vitro* embryoid body formation and *in vivo* teratoma assays revealed that the lines generate cell types of all three germ layers (Supplementary Fig. 12a online). Expression of pluripotency markers *TERC* and *TERT* and markers associated with full reprogramming *DNMT3B* and *REX1* were detected (Supplementary Fig. 12b online). Therefore CF-iPSC generated by retroviral-mediated reprogramming characteristically resembles hESC and are functionally pluripotent.

In order to sample the functional expression of CFTR in patches of epithelium we employed a modification of the iodide efflux[27] method for detecting regulated CFTR channel activity. The expression of the mature complex glycosylated form of CFTR “Band C” that represents the plasma membrane localized functional protein was detectable by Western blot analysis in hESC-derived but not in CF-iPSC-derived cultures (Fig. 4a). We then tested whether the *in vitro* differentiated epithelium from normal hESC and CF-iPSC (Supplementary Fig. 13 online) possessed cyclic AMP-regulated CFTR anion channel activity using a halide efflux assay. As expected from similar studies in epithelial cells endogenously expressing CFTR in their apical membranes, such as Caco-2 cells, cAMP agonists stimulated peak iodide efflux within 1–2 minutes in differentiated cultures (Figure 4b). There was heterogeneity with respect to the functional expression of CFTR in different cell lines, with two of the four ES cell lines exhibiting cAMP activated efflux. Of these two ES cell lines, one exhibited robust responses (red symbols in Figure 4c) similar to levels of control Caco-2 cells and the other, modest responses (green symbols). There was heterogeneity with respect to the efficacy of the differentiation protocol, with 2 of 4 differentiation trials leading to responsive cultures in the first cell line and 3 of 6 in the second cell line. The reasons for this variability have yet to be fully defined but likely reflect differential proportions of polarized CFTR-expressing epithelial cells in each culture. Nonetheless, this step-wise directed differentiation overcomes the previously encountered barriers to generating mature functional CFTR-expressing proximal airway epithelia.

In the F508del CF mutation, the mutant CFTR protein does not fold properly in the endoplasmic reticulum, preventing it from being properly trafficked to the plasma membrane. Instead the mutant protein is rapidly targeted for degradation[28]. Recent studies have shown that small molecules called “corrector” compounds are effective in partially rescuing the trafficking defect of the major mutant[29]. As a proof-of-concept to determine

whether CF-iPSC-derived epithelial cells may be used to evaluate novel CF corrector compounds, we tested the effect of C18, an active analog of the small molecule VX-809 (currently in phase II clinical trials) in promoting plasma membrane localization of F508del-CFTR in CF-iPSC-derived epithelial cells (Fig. 4d). Importantly, while no surface localized F508del-CFTR was detected in control DMSO-treated CF-iPSC-cultures, those cultures treated for 24 hours with C18 (10 μM) exhibited patches of cells expressing CFTR on their cell surface. Although we could not observe significant changes in cAMP-regulated iodide efflux from C18 treated cells (data not shown), we did observed a trend towards a change in the Band C to Band B ratio of F508del-CFTR protein in C18 treated cultures versus DMSO treated cultures from one F508del-CFTR proband (Figure 4e,f). Overall, CF-iPSC-derived airway cells may provide a novel renewable source of patient-specific cells to identify new or validate existing CF therapeutic drugs.

This is the first report to our knowledge demonstrating that human pluripotent stem cells can be directed to differentiate *in vitro* into CFTR-functional conducting airway epithelium. While the differentiation protocol generates heterogeneous endoderm lineages, a great majority of the cells express airway epithelia markers with CFTR functional establishment observed in a third of the cultures. Further refinement by isolating the cells using positive and negative selection or cell surface marker identification of lung progenitor populations would further generate pure populations of lung epithelial cells. This study also provides a proof-of-concept that CF-iPSC-derived epithelial cells may be used to validate existing or identify new therapeutic modulators of CFTR activity. Importantly this can be performed in a patient-specific manner, taking into account the genetic modifiers[30] that underlie the heterogeneity in F508del CF pathologies. Patient-specific iPSC-derived airway epithelial cells hold future promise of regenerative medicine approaches to treat serious lung diseases.

METHODS

Maintenance of pluripotent stem cells

Human ESC and iPSC were maintained on mitotically inactivated mouse embryonic fibroblast feeders in Knockout DMEM (GIBCO) with 15% Serum Replacement (GIBCO), Glutamax (Invitrogen), penicillin/streptomycin (GIBCO), 1 mM nonessential amino acids (GIBCO), 0.5 mM mercaptoethanol, and 10 ng/ml FGF2 (Peprotech). CA1, CA2 hESC were obtained from A. Nagy (Mount Sinai Hospital, Toronto, Canada). H9 hESC were obtained from The WiCell Research Institute (Wisconsin, USA). The hESC were cultured under the approval of the Canadian Institutes of Health Research Stem Cell Oversight Committee. Culture conditions for hESC cells are identical to those for hiPSC. To harvest cells for differentiation, hESC and iPSC colonies were dissociated with 0.25% trypsin (Invitrogen), washed with culture media and centrifuged to pellet the cells.

Differentiation of human ESC and iPSC into definitive endoderm

Differentiation into definitive endoderm was performed as previously described[7]. Briefly, pluripotent stem cells were harvested, gently triturated into single cell suspensions and seeded onto transwells (0.4μm pore size, Corning) pre-coated with human placental collagen Type IV, which has previously been shown to support airway epithelial cell growth[31]. The

cells were immediately treated with 100ng/ml Activin-A and 25ng/ml WNT3A (R&D Systems) for 4 consecutive days in Endoderm Differentiation Media consisting of serum-free Knockout DMEM (Invitrogen) with Glutamax (Invitrogen), penicillin/streptomycin (GIBCO), 1 mM nonessential amino acids (GIBCO) and 0.5 mM mercaptoethanol. Subsequent differentiation steps were performed on the transwells.

Differentiation of definitive endoderm into anterior foregut endoderm progenitors

For anterior foregut endoderm differentiation and especially embryonic lung progenitors, definitive endoderm cells were treated with 500ng/ml FGF2 (Preprotech) and 50ng/ml Sonic hedgehog (SHH, Cedarlane) for 5 days in Endoderm Differentiation Media. Extended culture with FGF2 and SHH did not significantly augment the number of NKX2.1+ cells generated.

Directed differentiation of foregut endoderm into mature lung cell fates

The cells were treated with 50ng/ml FGF10, 50ng/ml KGF (FGF7) and 5ng/ml BMP4 (all R&D systems) for 5 days followed by 10ng/ml FGF10, 10ng/ml FGF7 and 10ng/ml FGF18 (Sigma-Aldrich) for an additional 5 days. To differentiate the cells into mature airway epithelial cells, the cells were cultured in Bronchial Epithelial Growth Media (BEGM, Lonza) supplemented with FGF18 (10ng/ml) for 10 days followed by Bronchial-Air Liquid interface (B-ALI, Lonza) media for an additional 15+ days. The cells were “air-lifted” and B-ALI media was only added to the bottom but not the top of the transwell.

Generation and characterization of human iPSC lines

Human skin fibroblasts (GM00997, GM04320) were obtained from the Coriell Cell repository (Coriell Institute for Medical Research) and HSC patient fibroblast the Hospital for Sick Children (Toronto, Canada) with informed consent. These fibroblasts were isolated from the donor skin biopsy as previously described[26]. By 4 weeks of reprogramming obvious human ESC-like EGFP+ colony numbers were enriched under puromycin selection before picking and expansion. CF-iPSC lines with ESC-like morphology were further assessed for pluripotency marker expression (NANOG, TRA1-81, TRA1-60) by flow cytometry and immunofluorescence, and real-time qPCR to examine up-regulation of endogenous pluripotency genes (*OCT4, SOX2, C-MYC* and *KLF4*) and down-regulation of the exogenous retroviral transgenes. In addition, gene expression of other pluripotency markers DNMT3B, REX1, TERC, TERT were also assessed. Karyotype analysis was performed to determine genetic stability. Finally, iPSC lines were subjected to *in vitro* embryoid body and *in vivo* teratoma assays for functional tests of pluripotency as previously described[26].

Teratoma formation assay

Teratoma formation experiments were performed in NOD/SCID immunodeficient mice as previously described[26]. Human ESC (lines CA1, CA2 and H9) and mouse embryonic fibroblasts were used as positive and negative controls for experiment, respectively. All procedures using animals have been approved by the SickKids Animal Care Committee under the auspices of The Canadian Council on Animal Care.

Quantitative Real-time PCR

Total RNA was prepared using the RNeasy Kit (Qiagen). RNA was reverse transcribed for first-strand cDNA using Superscript II (Invitrogen) according to manufacturer's protocol. Quantitative real-time PCR (SYBR green detection method; Applied Biosystems, Foster City, CA) was performed for amplification of the genes listed in Table 1. Real-time PCR (45 cycles of amplification) was performed on the LightCycler® 480 System (Roche). Gene expression was normalized to the housekeeping gene β-ACTIN and expressed relative to a positive control sample. Denaturing curves for each gene were used to confirm DNA product and eliminate possibility of pseudogene amplification or primer-dimers. All experiments were done in triplicates with at least 3 separate differentiation cultures. Primer sequences are listed in Supplementary Table 1 and positive control tissue RNA listed in Supplementary Table 2 online.

Immunofluorescence

Transwells were fixed with fresh paraformaldehyde (4%) for 1 hour at room temperature. For CFTR staining, transwells were fixed with ice-cold methanol (100%) in −20ºC for 10 minutes. For cytoplasmic or nuclear stains, cells were permeabilized and blocked with a solution containing 0.25% Triton-X100 (Invitrogen), 2% BSA and 5–10% normal goat or donkey serum. Primary antibodies used are listed in Supplementary Table 3 online. Secondary antibodies include goat anti-rabbit, mouse or rat (IgG,) or donkey anti-goat IgG Alexa Fluor 488 and 555 (Molecular Probes). Nuclei were counterstained with DAPI (Invitrogen). Stains were visualized with the Confocal Digital Imaging System (Nikon) and analyzed with Volocity Software (PerkinElmer). Images were digitally processed using Adobe Photoshop CS5 (Adobe) in accordance with Nature Publishing Guidelines by altering only contrast and brightness.

Flow cytometry

Flow cytometry staining was performed as per manufacturer's protocol. For intracellular staining, cells were permeabilized with permeabilization (PERM) buffer containing saponin (BD Biosciences). For non-intracellular flow, the cells were resuspended and stained in FACS buffer containing 0.2% BSA. Primary antibodies used are listed in Supplementary Table 2. Secondary antibodies used include goat anti-mouse (IgG or IgM) or goat anti-rabbit (IgG,) Alexa Fluor 488, 647 (Molecular Probes) or PE-Cy7 (BD Biosciences). Non-immune reactive isotypes were used as staining controls. Data acquisition was performed using the LSRII flow cytometer (BD Biosciences) and analyzed with Flowjo software (Tree Star Inc).

Iodide efflux assay

A. Iodide loading and washing—Cells were loaded with 850 μl of NaI solution [3.0 mM KNO_3, 2.0 mM $Ca(NO_3)_2$, 11 mM glucose, 20 mM Hepes, 136 mM NaI] from the bottom of transwells at 37°C for 1 h for iodide uptake in cells. Resultant iodide solution was washed out 10 times with 4 ml of washing solution containing nitrate [3.0 mM KNO_3, 2.0 mM $Ca(NO_3)_2$, 11 mM glucose, 20 mM Hepes, 136 mM $NaNO_3$] and 100 μM amiloride, an epithelial sodium channel (ENaC) specific inhibitor was added.

B. cAMP-stimulated halide flux—The following time course used 350 μl of respective solution which was added to the top of transwells and then transferred to a 96-well plate well at each one minute time point. Time course for each culture involved: 3 min wash with washing solution and 8 min cAMP-stimulated halide flux with cAMP agonists, forskolin (10 μM) and 3-isobutyl-1-methylxanthine (100 μM, IBMX), and a CFTR potentiator, genistein (50 μM) in washing solution. Vehicle dimethyl sulfoxide (DMSO) served as the negative control. Since it has been known that Caco-2 can recapitulate properties of fully differentiated epithelia which include apical expression of CFTR and CFTR-mediated vectorial transepithelial chloride flux at 3–5 days post-confluency[32], cells were grown to 5 days post-confluency and then used for the functional discontinuous iodide efflux assay. Caco-2 cells were split and plated on 12-well dish (with each well approximately 3.8 cm^2 in area) coated with collagen IV prior to measurement.

C. Measurement and calibration—The halide-selective microelectrode (Lazar Research Laboratories, Los Angeles, CA) was used to measure the absolute iodide electrode potential (mV) value. Readings were recorded using the Digidata 1320A Data Acquisition System with the Clampex 8.1 program. A calibration curve was created by measuring the mV values of nitrate solutions containing 2 μM to 1 mM iodide to convert mV values to iodide concentration (μM).

Immunoblotting

Cells were solubilized in 1% sodium dodecyl sulphate (SDS) and sample protein run on 6% SDS gels for SDS-polyacrylamide gel electrophoresis. Protein samples were transferred to nitrocellulose paper. Primary CFTR antibody (MAB1660 or antibody #450 courtesy of JR Riordan) and goat anti-mouse Ig HRP secondary antibody were used for immunoblotting. Immunoblot was exposed to enhanced chemiluminescence (ECL).

Proliferation Assay

BrdU incorporation was assessed by flow cytometry using the BD BrdU flow kit (catalog # 552598) and performed using manufacturer's protocol. Cells were incubated with BrdU for 24 hours before analysis.

Statistical analysis

Unless otherwise specified, for statistical analysis, unpaired t-tests were performed. When more than two groups were compared, one-way ANOVA was used followed by Dunnett's post-test if significance was observed. Results were expressed as mean ± SEM.

Supplementary Material

Refer to Web version on PubMed Central for supplementary material.

Acknowledgments

We would like to thank Dr. Shinya Yamanaka (CiRA, Kyoto, Japan) and Dr. Andras Nagy (Samuel Lunenfeld Research Institute, Toronto, Canada) for providing human iPS lines (201B7, 253G1 and PB-4Fout respectively). We would also like to thank Dr. Robert Bridges (Rosalind Franklin University, Chicago, USA) who provided the C18 analog. This work was funded by an Emerging Team grant from the Canadian Institutes of Health Research

(GPG-102171) to CB, FR, JE and JR. This work was supported (in part) by an Ontario Ministry of Economic Development and Innovation (MEDI) grant. APW was a recipient of the MEDI Post-doctoral Award.

References

1. Van Haute L, De Block G, Liebaers I, Sermon K, De Rycke M. Generation of lung epithelial-like tissue from human embryonic stem cells. Respir Res. 2009; 10:105. [PubMed: 19891764]
2. Samadikuchaksaraei A, et al. Derivation of distal airway epithelium from human embryonic stem cells. Tissue Eng. 2006; 12:867–875. [PubMed: 16674299]
3. Wang D, Haviland DL, Burns AR, Zsigmond E, Wetsel RA. A pure population of lung alveolar epithelial type II cells derived from human embryonic stem cells. Proc Natl Acad Sci U S A. 2007; 104:4449–4454. [PubMed: 17360544]
4. Mou H, et al. Generation of Multipotent Lung and Airway Progenitors from Mouse ESCs and Patient-Specific Cystic Fibrosis iPSCs. Cell Stem Cell. 2012; 10:385–397. [PubMed: 22482504]
5. Kimura J, Deutsch GH. Key mechanisms of early lung development. Pediatr Dev Pathol. 2007; 10:335–347. [PubMed: 17929994]
6. Zorn AM, Wells JM. Vertebrate endoderm development and organ formation. Annu Rev Cell Dev Biol. 2009; 25:221–251. [PubMed: 19575677]
7. D'Amour KA, et al. Efficient differentiation of human embryonic stem cells to definitive endoderm. Nat Biotechnol. 2005; 23:1534–1541. [PubMed: 16258519]
8. Ameri J, et al. FGF2 specifies hESC-derived definitive endoderm into foregut/midgut cell lineages in a concentration-dependent manner. Stem Cells. 2010; 28:45–56. [PubMed: 19890880]
9. Serls AE, Doherty S, Parvatiyar P, Wells JM, Deutsch GH. Different thresholds of fibroblast growth factors pattern the ventral foregut into liver and lung. Development. 2005; 132:35–47. [PubMed: 15576401]
10. Bellusci S, et al. Involvement of Sonic hedgehog (Shh) in mouse embryonic lung growth and morphogenesis. Development. 1997; 124:53–63. [PubMed: 9006067]
11. Kim SK, Melton DA. Pancreas development is promoted by cyclopamine, a hedgehog signaling inhibitor. Proc Natl Acad Sci U S A. 1998; 95:13036–13041. [PubMed: 9789036]
12. Pan Q, et al. In vivo characterization of the Nkx2.1 promoter/enhancer elements in transgenic mice. Gene. 2004; 331:73–82. [PubMed: 15094193]
13. Bellusci S, Grindley J, Emoto H, Itoh N, Hogan BL. Fibroblast growth factor 10 (FGF10) and branching morphogenesis in the embryonic mouse lung. Development. 1997; 124:4867–4878. [PubMed: 9428423]
14. Shiratori M, et al. Keratinocyte growth factor and embryonic rat lung morphogenesis. Am J Respir Cell Mol Biol. 1996; 15:328–338. [PubMed: 8810636]
15. Morrisey EE, Hogan BL. Preparing for the first breath: genetic and cellular mechanisms in lung development. Dev Cell. 2010; 18:8–23. [PubMed: 20152174]
16. Weaver M, Yingling JM, Dunn NR, Bellusci S, Hogan BL. Bmp signaling regulates proximal-distal differentiation of endoderm in mouse lung development. Development. 1999; 126:4005–4015. [PubMed: 10457010]
17. Desai TJ, et al. Distinct roles for retinoic acid receptors alpha and beta in early lung morphogenesis. Dev Biol. 2006; 291:12–24. [PubMed: 16427040]
18. Metzler MD, Snyder JM. Retinoic acid differentially regulates expression of surfactant-associated proteins in human fetal lung. Endocrinology. 1993; 133:1990–1998. [PubMed: 8404646]
19. Whitsett JA, et al. Fibroblast growth factor 18 influences proximal programming during lung morphogenesis. J Biol Chem. 2002; 277:22743–22749. [PubMed: 11927601]
20. Rock JR, et al. Basal cells as stem cells of the mouse trachea and human airway epithelium. Proc Natl Acad Sci U S A. 2009; 106:12771–12775. [PubMed: 19625615]
21. Hong KU, Reynolds SD, Watkins S, Fuchs E, Stripp BR. In vivo differentiation potential of tracheal basal cells: evidence for multipotent and unipotent subpopulations. Am J Physiol Lung Cell Mol Physiol. 2004; 286:L643–649. [PubMed: 12871857]

22. Minoo P, et al. Physical and functional interactions between homeodomain NKX2.1 and winged helix/forkhead FOXA1 in lung epithelial cells. Mol Cell Biol. 2007; 27:2155–2165. [PubMed: 17220277]
23. Davies JR, Kirkham S, Svitacheva N, Thornton DJ, Carlstedt I. MUC16 is produced in tracheal surface epithelium and submucosal glands and is present in secretions from normal human airway and cultured bronchial epithelial cells. Int J Biochem Cell Biol. 2007; 39:1943–1954. [PubMed: 17604678]
24. Huang TH, et al. Control of keratin gene expression by vitamin A in tracheobronchial epithelial cells. Am J Respir Cell Mol Biol. 1994; 10:192–201. [PubMed: 7509163]
25. Ratjen F, Doring G. Cystic fibrosis. Lancet. 2003; 361:681–689. [PubMed: 12606185]
26. Hotta A, et al. EOS lentiviral vector selection system for human induced pluripotent stem cells. Nat Protoc. 2009; 4:1828–1844. [PubMed: 20010937]
27. Kim Chiaw P, Wellhauser L, Huan LJ, Ramjeesingh M, Bear CE. A chemical corrector modifies the channel function of F508del-CFTR. Mol Pharmacol. 2010; 78:411–418. [PubMed: 20501743]
28. Lewis HA, et al. Impact of the deltaF508 mutation in first nucleotide-binding domain of human cystic fibrosis transmembrane conductance regulator on domain folding and structure. J Biol Chem. 2005; 280:1346–1353. [PubMed: 15528182]
29. Van Goor F, et al. Correction of the F508del-CFTR protein processing defect in vitro by the investigational drug VX-809. Proc Natl Acad Sci U S A. 2011; 108:18843–18848. [PubMed: 21976485]
30. Wright FA, et al. Genome-wide association and linkage identify modifier loci of lung disease severity in cystic fibrosis at 11p13 and 20q13.2. Nat Genet. 2011; 43:539–546. [PubMed: 21602797]
31. Trinh NT, Prive A, Maille E, Noel J, Brochiero E. EGF and K+ channel activity control normal and cystic fibrosis bronchial epithelia repair. Am J Physiol Lung Cell Mol Physiol. 2008; 295:L866–880. [PubMed: 18757521]
32. Sood R, et al. Regulation of CFTR expression and function during differentiation of intestinal epithelial cells. EMBO J. 1992; 11:2487–2494. [PubMed: 1378393]

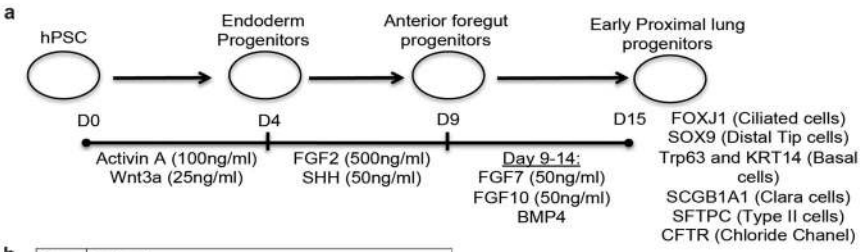

b

Group	Treatment
A	Undifferentiated PSC
B	Anterior foregut endoderm progenitor cells
C	+ FGF7 (50ng/ml) + FGF10 (50ng/ml)
D	+ FGF7 (50ng/ml) + FGF10 (50ng/ml) + BMP4 (5ng/ml)
E	+ FGF7 (50ng/ml) + FGF10 (50ng/ml) + BMP4 (10ng/ml)
F	+ FGF7 (50ng/ml) + FGF10 (50ng/ml) + BMP4 (50ng/ml)

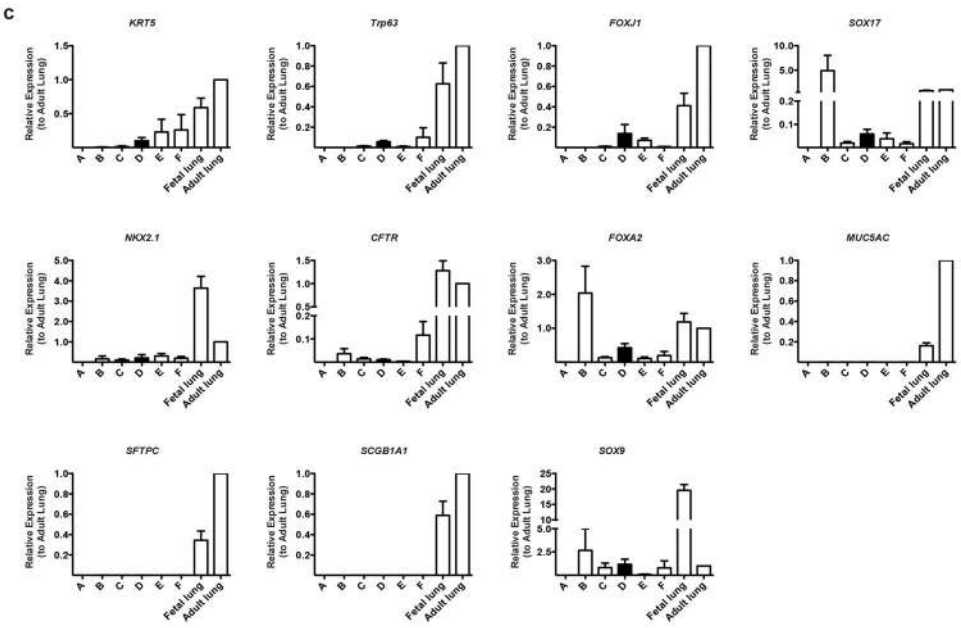

Figure 1. Low concentration of BMP4 up-regulates genes associated with early proximal lung progenitors

a–b. Differentiation to immature lung endoderm cells. **c.** Expression of airway genes such as *KRT5* and *Trp63* (basal cell marker), *FOXJ1* and *SOX17* (ciliated cell markers), *NKX2.1* (earliest marker of the lung endoderm), *CFTR* and the pan-endoderm marker *FOXA2* were up-regulated with 10ng/ml of BMP4 (treatment D). Other airway marker *MUC5AC* (goblet cell marker) was not detected. In addition, the Type II alveolar cell marker surfactant protein-C (SFTPC) and the Clara cell marker *SCGB1A1* were not detected up-regulated. *SOX9*, a marker of the distal tip progenitors found in the developing embryonic lung was also detected. Genes were normalized to the housekeeping gene *β-ACTIN* and expressed relative to adult tissue positive control RNA. Error bars are s.e.m (n=3 experiments).

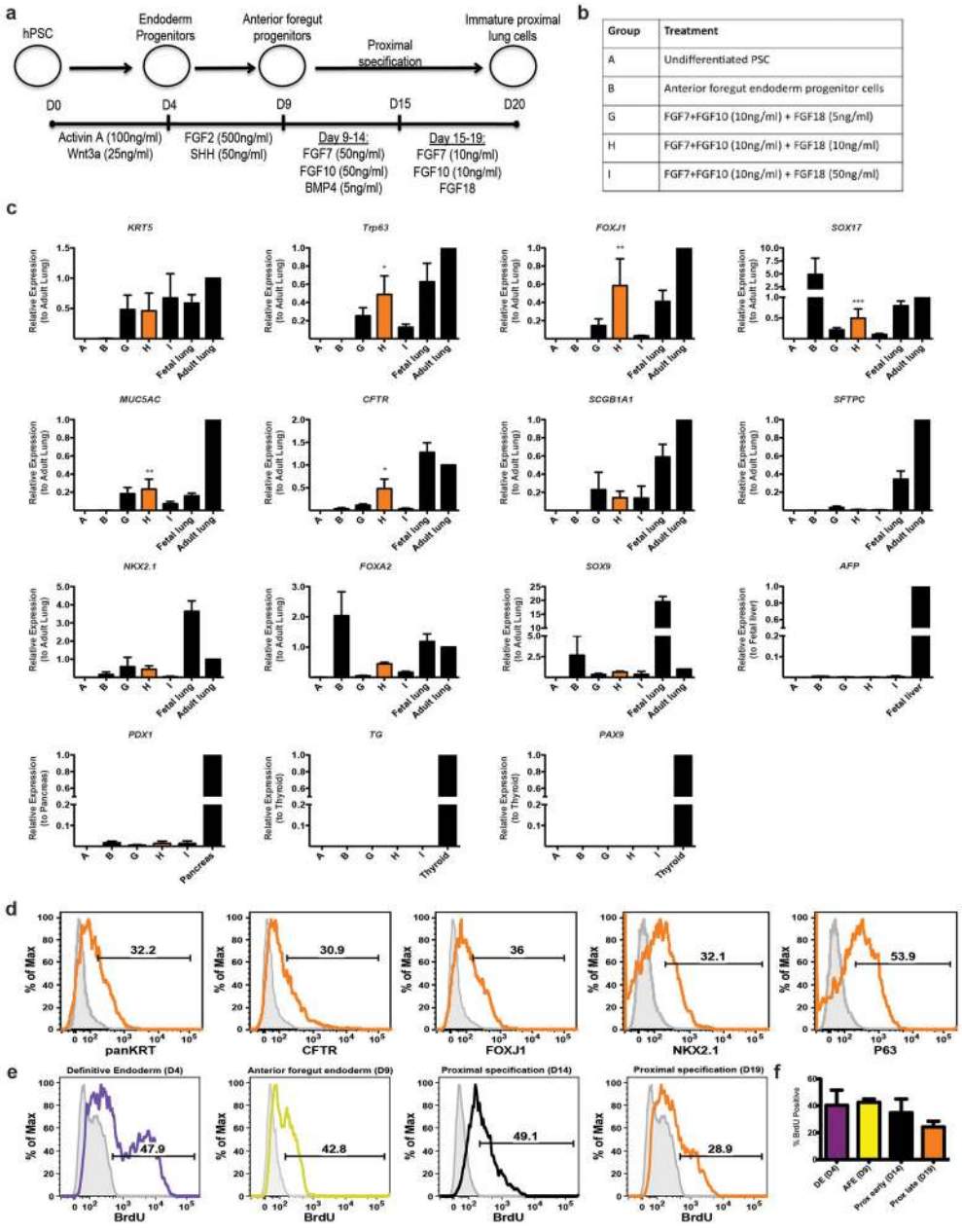

Figure 2. FGF18 promotes proximal airway epithelia formation

a–b. Differentiation to proximal lung cells. **c.** Expression of proximal lung cell genes *KRT5*, *Trp63*, *FOXJ1*, *SOX17*, *MUC5*, *CFTR*, were up-regulated with 10ng/ml of FGF18 (treatment H). Lower levels of the Clara cell marker *SCGB1A1*, and no significant detection of *SFTPC* were detected. Other endoderm lineage markers TG and *PAX9*, *AFP*, *PDX1* and *NKX6.1* were not up-regulated. The transcription factors *NKX2.1* and *FOXA2* that regulate *SCGB1A1* and *SFTPC* expression as well as the distal tip progenitor marker *SOX9* were down regulated (compared to B). Other endoderm lineage markers *AFP* (liver), *PDX1* (pancreas), *TG* (thyroid) and *PAX9* (pharyngeal endoderm) were not detected. **d.** Representative flow histograms of cells from treatment H reveal approximately one-third of

the cells are epithelial (panKRT+), CFTR+, FOXJ1+ and NKX2.1+. A majority of the cells express Trp63 (a homolog of p53 that initiates the stratified program in epithelial cells). Grey solid histograms represent respective isotype controls. **e.** Representative histograms of BrdU incorporation at different stages of differentiation. **f.** Average cell proliferation at different stages of differentiation from 4 independent lines. Genes were normalized to the housekeeping gene *β-ACTIN* and expressed relative to adult lung positive control RNA. Error bars are s.e.m (n=3 experiments). *P<0.01, **P<0.001, ***P<0.05 compared to treatment B.

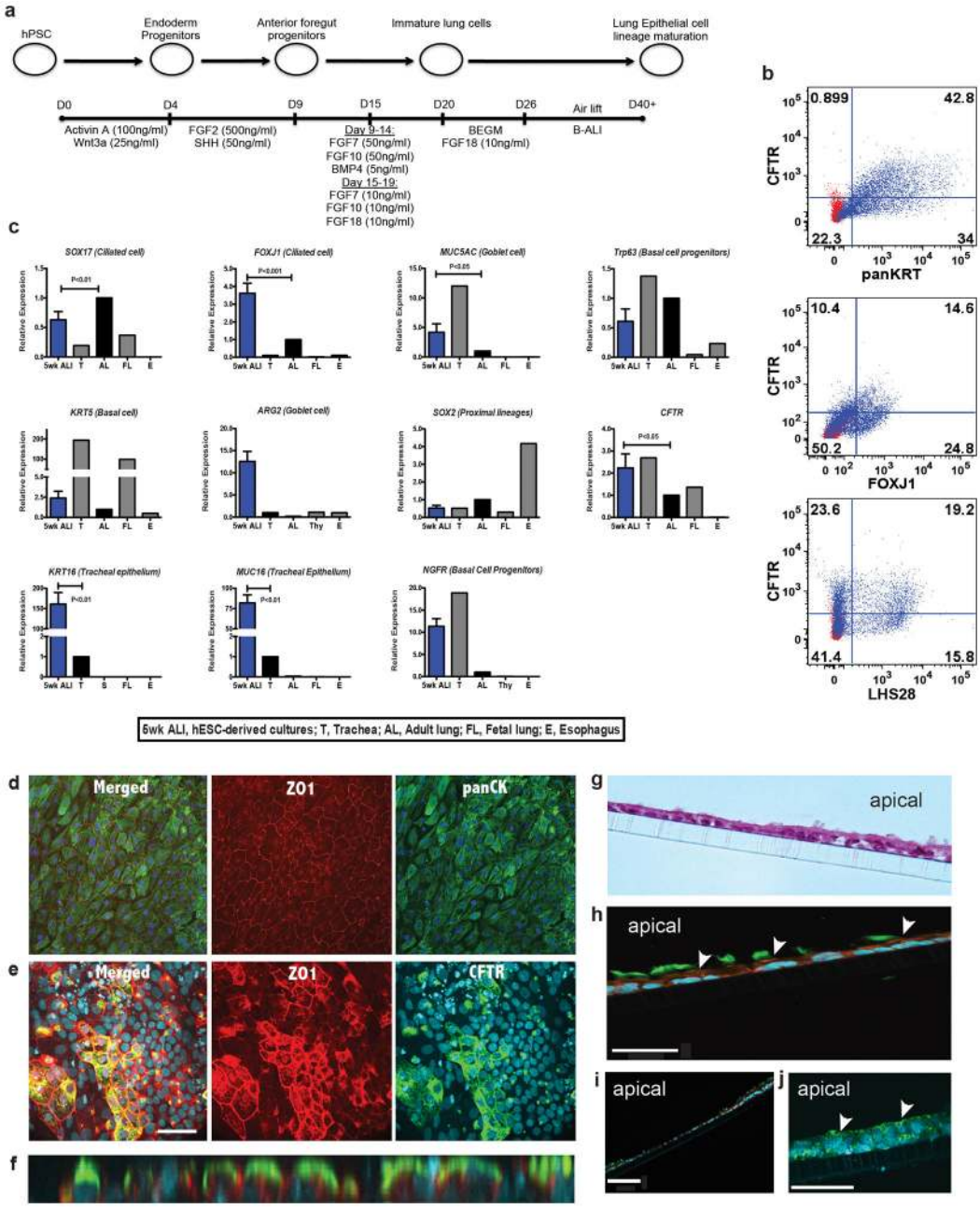

Figure 3. Air liquid interface induces airway epithelial cell differentiation and promotes apical expression of CFTR

a. Schematic of differentiation protocol to generate mature airway epithelium using air liquid interface to induce polarization and apical expression of CFTR as observed in mature airway epithelium. **b.** The percentage of CFTR+, panKRT+ and FOXJ1+ cells was higher after 3 weeks of ALI while the number of Trp63+ cells was dramatically reduced. **c.** Gene expression levels of airway markers *FOXJ1, MUC5AC, KRT5, Trp63* and *SOX17* were significantly higher or comparable to adult lung tissue. Noticeably, *CFTR* was also up-regulated. The Clara cell marker *SCGB1A1* and Type II alveolar cell marker *SFTPC* were not significantly up-regulated. Genes were normalized to *β-ACTIN* and expressed relative to

adult lung tissue positive control RNA. Error bars are s.e.m (n=3). *P<0.01, **P<0.001 compared to adult lung tissue. **d.** To confirm the cells are epithelial, co-staining for ZO1 and pan-cytokeratin marker (panKRT) confirmed co-localization of the two proteins suggesting establishment of a tight epithelium. **e.** Maximal intensity projections of Z-stack confocal images of a 5 week-old ALI culture of human ESC CA1 line-derived epithelia co-express the tight junction associated protein ZO1 and CFTR (clone L12B4). **f.** The X-Z planar view of the epithelium show apical localization of the CFTR protein. **g.** Hematoxylin and eosin staining show cilia on some cells. **h.** Higher magnification shows ciliated cells (green) and apical localization of CFTR (orange, white arrowheads point to apical CFTR). White bar represents 21 microns. **i.** Low magnification of an ALI transwell cross-section stained for cilia (beta IV tubulin, green) and CFTR (orange) show non-uniform growth of cells with areas of pseudostratified cells and areas of sparse monolayer cells. White bar represents 90 microns. **j.** High magnification of a culture stained for MUC5AC (green) on the surface of the cells (arrowheads). White bar represents 60 microns.

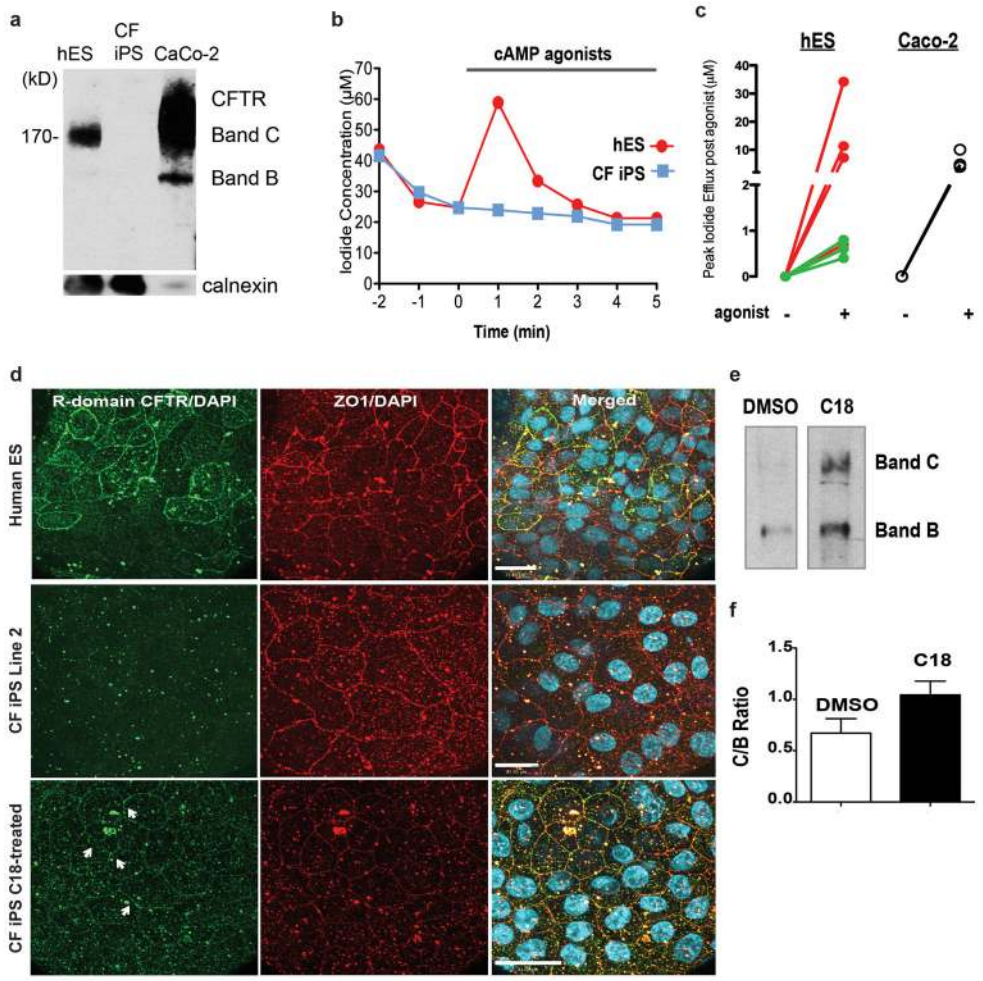

Figure 4. Establishment of functional CFTR hESC-derived airway epithelia and correction of CF phenotype in CF-iPSC-derived epithelial cells with a small molecule compound C18

a. Western blot shows Band C appearing (~170kDa) in 6-week old hESC-derived epithelial cells (the CA1 cell line) indicative of the complex glycosylated functional form of CFTR. As a positive control, Caco2, a human colorectal adenocarcinoma epithelial cell line that expresses endogenous CFTR was used. The antibody used in this Western (mAb #660) recognizes a peptides within NBD1 of CFTR). Calnexin was probed for loading control. An iodide efflux assay was performed to assess CFTR function in hESC-derived epithelial cells. The cells were preloaded with NaI and regulated CFTR channel activity was stimulated with the agonists of cyclic AMP including: forskolin (10 μM), isobutylmethyl xanthine (100 μM) and genistein (50 μM) (or VX-532 at 10 μM) to activate and potentiate CFTR channel open time at the cell surface. Iodide flux across the apical side of epithelial cells in ALI cultures reports CFTR channel activity since CFTR is permeable to iodide. Iodide efflux was measured using a iodide sensitive microelectrode. CFTR channel activity was detected as a change in iodide flux one to two minutes after addition of cAMP agonists in certain hESC cultures. **b.** Representative iodide flux graph shows cyclic AMP agonist induced CFTR activity in a differentiated hESC-derived 6-week old ALI culture but not in CF-iPSC-derived culture. **c.** The response to stimulation of CFTR in 2 hES cell lines, H9 (red) and CA1

(green) and control Caco-2 cell that line that expresses wild-type CFTR (black, 3 cultures). Each line represents a different responsive culture (i.e., showing an increase in efflux rate within 1–2- minutes of stimulation). Four H9 cultures were responsive from a total of 13 cultures and three CA1 cultures were responsive of 16 studied. The H9 cell line could be differentiated to exhibit relatively robust responses. **d.** Representative photomicrographs of hESC (CA1 line), CF-iPSC GM00997 Line 2 treated with either DMSO (control) or C18 (10μM) and co-stained for tight junction-associated protein ZO1 and CFTR. This antibody recognizes an epitope in the R-domain. Plasma membrane localization of CFTR was observed (white arrowheads) after 2 days of treatment with C18 in the CF-iPSC-derived epithelial cells but not in DMSO controls. White bar indicates scale in microns. **e.** Cropped western blot shows the accumulation of Band C (mature complex glycosylated form) in C18-corrected cells while the predominant form of the mutant protein in uncorrected cells is Band B (core-glycosylated, ER-retained protein). The antibody used in this Western (mAb #450) recognizes the CFTR peptide: 698-705). Full length blots are presented in Supplementary Figure 14. We observed a trend towards an increase in the C (complex glycosylated) to B ratio of F508del-CFTR protein in C18 treated cultures (n=4) versus DMSO treated cultures (n=3, **f.)**